Effect of pulse temporal shape on optical trapping and impulse transfer using ultrashort pulsed lasers

Janelle C Shane[1,2,3], Michael Mazilu[1,3]*, Woei Ming Lee[1], Kishan Dholakia[1]

[1] *SUPA, School of Physics and Astronomy, University of St Andrews, St Andrews, Fife KY16 9SS, United Kingdom*

[2] *Current address: Department of Electrical and Computer Engineering, University of California at San Diego, La Jolla, CA 92093-0407, USA*

[3] *These authors contributed equally to this work.*

mm17@st-andrews.ac.uk

Abstract: We investigate the effects of pulse duration on optical trapping with high repetition rate ultrashort pulsed lasers, through Lorentz-Mie theory, numerical simulation, and experiment. Optical trapping experiments use a 12 femtosecond duration infrared pulsed laser, with the trapping microscope's temporal dispersive effects measured and corrected using the Multiphoton Intrapulse Interference Phase Scan method. We apply pulse shaping to reproducibly stretch pulse duration by 1.5 orders of magnitude and find no material-independent effects of pulse temporal profile on optical trapping of 780nm silica particles, in agreement with our theory and simulation. Using pulse shaping, we control two-photon fluorescence in trapped fluorescent particles, opening the door to other coherent control applications with trapped particles.

OCIS codes: (140.7010) Laser trapping, (320.5540) Pulse shaping

References and links

1. K. C. Neuman and S. M. Block, "Optical trapping," Rev. Sci. Instrum. **75**, 2787–2809 (2004).
2. K. Dholakia, P. Reece, and M. Gu, "Optical micromanipulation," Chem. Soc. Rev. **37**, 42–55 (2008).
3. K. Dholakia, M. P. MacDonald, P. Zemanek, and T. Cižmár, "Cellular and colloidal separation using optical forces" in "Laser manipulation of cells and tissues methods in cell biology," M. Berns and K. Greulich, ed., **82**, 467–495 (Elsevier, 2007).
4. G. C. Spalding, J. Courtial, and R. D. Leonardo, "Holographic optical tweezers," in "Structured Light and its Applications: An Introduction to Phase-Structured Beams and Nanoscale Optical Forces," D. L. Andrews, ed., 139–168, (Elsevier, 2008).
5. K. Dholakia and W. M. Lee, "Optical trapping takes shape: the use of structured light fields," Adv. Atomic, Molecular, Opt. Physics **56**, 261–337 (2008).
6. H. Misawa, M. Koshioka, K. Sasaki, N. Kitamura, and H. Masuhara, "Three-dimensional optical trapping and laser ablation of a single polymer latex particle in water," J. Appl. Phys. **70**, 3829 (1991).
7. L. Malmqvist and H. M. Hertz, "2nd-harmonic generation in optically trapped nonlinear particles with pulsed lasers," Appl. Opt. **34**, 3392–3397 (1995).
8. E. V. Perevedentseva, A. V. Karmenyan, F. J. Kao, and A. Chiou, "Second harmonic generation of biotin and biotin ester microcrystals trapped in optical tweezers with a mode-locked Ti : Sapphire laser," Scanning **26**, I78–I82 (2004).

#123223 - $15.00 USD Received 25 Jan 2010; revised 9 Mar 2010; accepted 11 Mar 2010; published 26 Mar 2010

9. B. Agate, C. T. A. Brown, W. Sibbett, and K. Dholakia, "Femtosecond optical tweezers for in-situ control of two-photon fluorescence," Opt. Express **12**, 3011–3017 (2004).
10. K. Dholakia, H. Little, C. T. A. Brown, B. Agate, D. McGloin, L. Paterson, and W. Sibbett, "Imaging in optical micromanipulation using two-photon excitation," New J. Phys. **6**, 136 (2004).
11. A. Fontes, K. Ajito, A. A. R. Neves, W. L. Moreira, A. A. de Thomaz, L. C. Barbosa, A. M. de Paula, and C. L. Cesar, "Raman, hyper-Raman, hyper-Rayleigh, two-photon luminescence and morphology-dependent resonance modes in a single optical tweezers system," Phys. Rev. E **72**, 012903 (2005).
12. N. K. Metzger, E. M. Wright, W. Sibbett, and K. Dholakia, "Visualization of optical binding of microparticles using a femtosecond fiber optical trap," Opt. Express **14**, 3677–3687 (2006).
13. D. Morrish, X. S. Gan, and M. Gu, "Morphology-dependent resonance induced by two-photon excitation in a micro-sphere trapped by a femtosecond pulsed laser," Opt. Express **12**, 4198–4202 (2004).
14. D. Morrish, X. S. Gan, and M. Gu, "Scanning particle trapped optical microscopy based on two-photon-induced morphology-dependent resonance in a trapped microsphere," Appl. Phys. Lett. **88** (2006).
15. S. Kuriakose, D. Morrish, X. Gan, J. W. M. Chon, K. Dholakia, and M. Gu, "Near-field optical trapping with an ultrashort pulsed laser beam," Appl. Phys. Lett. **92**, 081108 (2008).
16. J. W. Chan, H. Winhold, S. M. Lane, and T. Huser, "Optical trapping and coherent anti-Stokes Raman scattering (CARS) spectroscopy of submicron-size particles," IEEE J. Sel. Top. Quantum Electron. **11**, 858–863 (2005).
17. K. Inaba, K. Imaizumi, K. Katayama, M. Ichimiya, M. Ashida, T. Iida, H. Ishihara, and T. Itoh, "Optical manipulation of CuCl nanoparticles under an excitonic resonance condition in superfluid helium," Physica Status Solidi B **243**, 3829–3833 (2006).
18. J. L. Deng, Q. Wei, Y. Z. Wang, and Y. Q. Li, "Numerical modeling of optical levitation and trapping of the stuck particles with a pulsed optical tweezers," Opt. Express **13**, 3673–3680 (2005).
19. A. A. Ambardekar and Y. Q. Li, "Optical levitation and manipulation of stuck particles with pulsed optical tweezers," Opt. Lett. **30**, 1797–1799 (2005).
20. L. Pan, A. Ishikawa, and N. Tamai, "Detection of optical trapping of CdTe quantum dots by two-photon-induced luminescence," Phys. Rev. B **75**, 161305 (2007).
21. L. Jauffred, A. C. Richardson, and L. B. Oddershede, "Three-dimensional optical control of individual quantum dots," Nano Lett. **8**, 3376–3380 (2008).
22. L.-G. Wang and C.-L. Zhao, "Dynamic radiation force of a pulsed Gaussian beam acting on a Rayleigh dielectric sphere," Opt. Express **15**, 10615–10621 (2007).
23. A. K. De, D. Roy, A. Dutta, and D. Goswami, "Stable optical trapping of latex nanoparticles with ultrashort pulsed illumination," Appl. Opt. **48**, G33–G37 (2009).
24. Y. Deng, J. Bechhoefer, and N. R. Forde, "Brownian motion in a modulated optical trap," J. Opt. A: Pure and Applied Optics **9**, S256–S263 (2007).
25. J. D. Jackson, *Classical Electrodynamics* (Wiley, 1998).
26. S. Stallinga, "Radiation force on a Fabry-Perot slab immersed in a dielectric," Opt. Express **14**, 1286–1295 (2006).
27. J. P. Gordon, "Radiation forces and momenta in dielectric media," Phys. Rev. A **8**, 14–21 (1973).
28. R. Loudon and S. M. Barnett, "Theory of the radiation pressure on dielectric slabs, prisms and single surfaces," Opt. Express **14**, 11855–11869 (2006).
29. M. Mansuripur, "Radiation pressure and the linear momentum of the electromagnetic field," Opt. Express **12**, 5375–5401 (2007).
30. I. Brevik, "Experiments in phenomenological electrodynamics and the electromagnetic energy-momentum tensor," Phys. Reports **52**, 133–201 (1979).
31. M. Dienerowitz, M. Mazilu, and K. Dholakia, "Optical manipulation of nanoparticles: a review," J. Nanophotonics **2**, 021875 (2008).
32. F. Gittes and C. F. Schmidt, "Interference model for back-focal-plane displacement detection in optical tweezers," Opt. Lett. **23**, 7–9 (1998).
33. V. V. Lozovoy, I. Pastirk, and M. Dantus, "Multiphoton Intrapulse Interference. IV. Ultrashort laser pulse spectral phase characterization and compensation," Opt. Lett. **29**, 775–777 (2004).
34. B. Xu, J. M. Gunn, J. M. D. Cruz, V. V. Lozovoy, and M. Dantus, "Quantitative investigation of the Multiphoton Intrapulse Interference Phase Scan method for simultaneous phase measurement and compensation of femtosecond laser pulses," J. Opt. Soc. Am. B **23**, 750–759 (2006).
35. M. Dantus, V. V. Lozovoy, and I. Pastirk, "MIIPS characterizes and corrects femtosecond pulses," Laser Focus World **43**, 101–104 (2007).
36. J. Shane, M. Mazilu, W. M. Lee, and K. Dholakia, "Optical trapping using ultrashort 12.9fs pulses," Optical Trapping and Optical Micromanipulation V, Proc. SPIE, **7038**, 70380Y (2008).
37. K. Svoboda and S. M. Block, "Biological applications of optical forces," Annual Reviews in Biophysics and Biomolecular Structure **23**, 247–285 (1994).
38. N. Dudovich, D. Oron, and Y. Silberberg, "Single-pulse coherently controlled nonlinear Raman spectroscopy and microscopy," Nature **418**, 512–514 (2002).
39. Y. Coello, B. Xu, T. Miller, V. Lozovoy, and M. Dantus, "Group-velocity dispersion measurements of water,

#123223 - $15.00 USD Received 25 Jan 2010; revised 9 Mar 2010; accepted 11 Mar 2010; published 26 Mar 2010

seawater, and ocular components using Multiphoton Intrapulse Interference Phase Scan," Appl. Opt. **46**, 8394–8401 (2007).
40. V. V. Lozovoy, B. Xu, J. C. Shane, and M. Dantus, "Selective nonlinear optical excitation with pulses shaped by pseudorandom Galois fields," Phys. Rev. A **74**, 41805 (2006).
41. J. M. Dela Cruz, I. Pastirk, M. Comstock, V. V. Lozovoy, and M. Dantus, "Use of coherent control methods through scattering biological tissue to achieve functional imaging," Proc. Natl. Acad. Sci., USA **101**, 16996–7001 (2004).

1. Introduction

The exertion of forces upon mesoscopic particles by optical fields has been at the heart of many advances across all of the sciences in the last four decades. In particular, optical trapping allows the contact-free manipulation of microparticles by light. The calibratable nature of such optical traps has enabled ultra-precise measurements of the dynamics of macromolecules[1]. More generally optical forces may be used for studies within microfluidic environments, of fundamental aspects of optical fields and their angular momentum and within cell biology[2]. Extending the number and form of each optical trap can lead to the generation of potential energy landscapes. The interplay of optical forces and those from fluid flow and hydrodynamics may lead to the realization of optical sorting[3]. Extending the number and form of each optical trap can lead to the generation of potential energy landscapes. Such landscapes may be created by the use of rapidly scanning the incident light field (i.e. time-sharing the trapping beam) or they may be created interferometrically using diffractive optical elements, for example spatial light modulators[4, 5].

A set of key choices lie at the heart of a basic optical tweezers system: in addition to the high numerical aperture objective lens used to obtain a tightly focussed beam, the choice of laser is crucial. Naturally the choice of laser wavelength is critical for minimising damage to the trapped particle: this is particularly pertinent when considering biological material. Thus the most widely used laser sources have typically been continuous-wave (CW) near-infrared lasers. However, the last decade has seen an increasing use of pulsed and broadband lasers instead of, or in addition, to CW sources. This potentially offers the ability to observe nonlinear effects or perform spectroscopy in combination with optical trapping. Pulsed lasers offer extremely high peak powers at lower average powers, and therefore allow access to multiphoton processes that would otherwise require very high average powers. These effects become dramatic for ultrashort pulsed lasers, typically employing lasers in the femtosecond region of 100fs or less in pulse duration. A range of experiments have been performed exploiting these properties[6-17].

The very nature and form of the optical forces generated from pulsed lasers versus their CW counterparts remains an interesting topic in the literature. The peak power of a pulsed laser source has been used in separating stuck particles from surfaces. This phenomenon was theoretically modelled in a paper by Deng et al[18], who calculated that the peak gradient force during a laser pulse was enough to overcome the binding interaction between a particle and a glass surface. Ambardekar et al used a microsecond pulsed laser to separate adsorbed 2μm polystyrene beads and yeast cells from their substrates[19], which they attributed to the high peak gradient force of their pulsed laser. Pan et al used a picosecond pulsed laser source of 120-140mW average power for axial guiding and 2D trapping of clumps of 3-4nm quantum dots[20]. Although they showed no experimental data attempting to trap the quantum dots with a CW source of the same average power, they calculated that trapping would be not possible in a CW source of less than 20W power. Their calculations demonstrate the impressive peak gradient forces created by pulsed lasers, but only consider peak trapping force, not total trapping force over the laser's repetition period. An alternate explanation of their success in optical trapping might be the presence of optical binding effects within the clusters of trapped quantum

#123223 - $15.00 USD Received 25 Jan 2010; revised 9 Mar 2010; accepted 11 Mar 2010; published 26 Mar 2010

dots. It is to be noted that related experiments trapped quantum dots using continuous wave light sources subsequent to this work[21].

Wang and Zhao explored theoretically the trapping of Rayleigh sized particles with pulsed lasers and also calculated an extremely high peak force[22], especially in the axial direction, although they did not examine total momentum tranfer over a pulse's repetition cycle. Their calculations indicated no major material dependence or wavelength dependence. An experimental comparison of the trapping force for a CW source and a pulsed femtosecond laser of the same average power was reported in 2004 by Agate et al.[9]. They recorded Q values for the trapped 1.28μm silica microspheres and found no appreciable difference between them for the cases of a CW source and the pulsed laser source, for trapping. Most recently a study has shown stable optical trapping of nanoparticles with a pulsed laser field[23]. Thus some results in the literature indicate that there may be a difference in trapping with CW versus trapping with pulsed light fields. Naturally the high peak powers of pulsed lasers allow access to material-dependent or medium-dependent nonlinear processes, which may have an appreciable effect on optical micromanipulation. To date there remains an uncertainty as to whether there are material-independent optical trapping effects that depend on peak power rather than average power; that is, whether pulsed lasers behave differently from CW lasers in optical trapping. If optical trapping is independent of the laser's temporal characteristics, then it should be possible to use advanced pulse shaping methods for spectroscopic techniques on trapped particles, without affecting the trapping process itself. Here we aim to address this question.

We present a detailed theory for optical trapping that is applicable at all size scales for a trapped particle with respect to the trapping laser pulse duration. We consider the case where the laser repetition rate is high enough to ignore any artifacts due to particle diffusion. Our theoretical derivation shows no effect on trapping efficiency due to pulse duration. By implementing an in situ pulse compression system in conjunction with a 12fs source we experimentally support this conclusion by determining trap stiffness for trapped dielectric microparticles for pulse durations ranging from 12fs to 500fs and show no appreciable difference. In addition to the high peak powers, a significant feature of ultrashort pulses is their broad bandwidths that may be used for pulse shaping: ultrashort lasers with carefully controlled spectral phase across their broad bandwidths are used to produce highly-selective nonlinear effects. We conclude by demonstrating the first use of pulse shaping in conjunction with optical trapping, exploring two-photon excitation in dyed trapped microspheres.

2. Theory

This section outlines theoretical arguments demonstrating that optical trapping does not depend on the duration of a pulsed laser, but only on the laser's frequency spectrum. In other words, trapping with a pulsed laser source should be equivalent to trapping with a CW laser source with the same bandwidth and average power. Here, we assume that pulse repetition rate is high enough that the particle does not diffuse significantly between pulses; for very low (less than around 1kHz) repetition rates, external effects such as Brownian motion will play a role[24]. We also assume that scattering is not intensity dependent.

2.1. Momentum and impulse transfer

Consider a laser pulse whose electric and magnetic fields $\mathbf{E}(x,y,z,t)$ and $\mathbf{H}(x,y,z,t)$ are both position, time-dependent and real. Assuming that the electric and magnetic fields have the same time dependence, we can decompose the pulse into two separate parts as follows:

#123223 - $15.00 USD Received 25 Jan 2010; revised 9 Mar 2010; accepted 11 Mar 2010; published 26 Mar 2010

$$\begin{aligned}\mathbf{E}(x,y,z,t) &= \mathscr{E}(x,y,z)a(t)\\ \mathbf{H}(x,y,z,t) &= \mathscr{H}(x,y,z)a(t)\end{aligned} \tag{1}$$

In the frequency domain these are expressed as:

$$\begin{aligned}\mathbf{E}(x,y,z,t) &= \mathscr{E}(x,y,z)\int_{-\infty}^{\infty}\hat{a}(\omega)e^{-i\omega t}d\omega\\ \mathbf{H}(x,y,z,t) &= \mathscr{H}(x,y,z)\int_{-\infty}^{\infty}\hat{a}(\omega)e^{-i\omega t}d\omega\end{aligned} \tag{2}$$

where, $\hat{a}(\omega)$ is the Fourier transform of $a(t)$. The effect of the pulse on the scattering particle is defined by the electromagnetic force density

$$f_i = \partial_j T_{ij} - \partial_t g_i \tag{3}$$

which gives us the amount of force exerted by the laser pulse's electromagnetic field in an infinitesimally small volume within the particle, at a given point in time. We write these expressions in compact form using Einstein summation convention. In this convention, writing $\partial_j T_{ij}$ is equivalent to writing $\sum_{j=1,3}\partial_j T_{ij} = \partial_x T_{ix} + \partial_y T_{iy} + \partial_x T_{iz}$ [25, 26]. f_i is composed of two terms, both dealing with momentum transfer from the pulse to the particle (as evidenced by a change in momentum or in momentum density). The first term corresponds to Maxwell's stress tensor and defines the influx of optical momentum per unit of time

$$T_{ij} = E_i D_j + H_i B_j - \frac{1}{2}\delta_{ij}(E_k D_k + H_k B_k) \tag{4}$$

and the second term arises from the variation in electromagnetic momentum density

$$g_i = \varepsilon_{ijk} D_j B_k \tag{5}$$

Here, $D_i = \varepsilon_r \varepsilon_0 E_i$ (electric displacement), and $B_i = \mu_r \mu_0 H_i$ (magnetic flux). ε_r is the relative dielectric constant, ε_0 is the permittivity of free space, μ_r is the relative permeability, and μ_0 is the permeability of free space. Here ε_{ikl} is the Levi-Civita totally antisymmetric pseudo-tensor of third rank defined by $\varepsilon_{ijk} = \mathrm{sgn}(i-j)\,\mathrm{sgn}(j-k)\,\mathrm{sgn}(k-i)$ with the function sgn representing the sign function.

To calculate the total optical force exerted by the pulse on the entire particle, over the entire duration of the pulse, we need to integrate equation (3) over the particle's volume, and over time. So that we may discuss the answer in terms of average force exerted, instead of assuming a single pulse and integrating from $-\infty$ to $+\infty$, we assume a train of pulses where the pulse repetition period Δt is much larger than the pulse duration. The momentum density g_i term of f_i cancels out during this integration:

$$\int_0^{\Delta t}\partial_t g_i dt = g_i(\Delta t) - g_i(0) \tag{6}$$

and $g_i(\Delta t) = g_i(0)$ since there is no field at time 0 and Δt. We are left with an expression for the average optical force that contains only the T_{ij} term:

$$\begin{aligned}< F_i > &= \frac{1}{\Delta t}\int_0^{\Delta t} f_i dV dt\\ &= \frac{1}{\Delta t}\int_0^{\Delta t}\int_S T_{ij} ds_j dt\end{aligned} \tag{7}$$

#123223 - $15.00 USD Received 25 Jan 2010; revised 9 Mar 2010; accepted 11 Mar 2010; published 26 Mar 2010

The second equation includes a surface integral evaluated on a closed surface S surrounding the particle, with $ds_j = n_j ds$ being a unit vector normal to the surface pointing outwards. Inserting equation (4) into equation (7) gives us

$$\begin{aligned} < F_i > &= \frac{1}{\Delta t}\int_S\int_0^{\Delta t} T_{ij} dt ds_j & (8)\\ &= \frac{1}{\Delta t}\int_S\int_0^{\Delta t}\left[E_i D_j + H_i B_j - \frac{1}{2}\delta_{ij}(E_k D_k + H_k B_k)\right] dt ds_j & (9)\\ &= \frac{1}{\Delta t}\left[\int_S\int_0^{\Delta t} E_i D_j dt ds_j + \int_S\int_0^{\Delta t} H_i B_j dt ds_j + \ldots\right] & (10)\end{aligned}$$

Next, we examine the first term in equation (10). Similar arguments will hold for all the other terms as they are all quadratic in the electric and magnetic field components. Using equation (2), this term can be rewritten as

$$\begin{aligned}\int_S\int_0^{\Delta t} E_i D_j dt ds_j &= \varepsilon_r\varepsilon_0\int_S\int_0^{\Delta t} E_i E_j dt ds_j\\ &= \varepsilon_r\varepsilon_0\int_S\int_0^{\Delta t}\left(\mathscr{E}_i\int_{-\infty}^{\infty}\hat{a}(\omega_1)e^{-i\omega_1 t}d\omega_1\right)\left(\mathscr{E}_j\int_{-\infty}^{\infty}\hat{a}(\omega_2)e^{-i\omega_2 t}d\omega_2\right)dt ds_j\\ &= \varepsilon_r\varepsilon_0\int_S\mathscr{E}_i\mathscr{E}_j\int_{-\infty}^{\infty}\int_{-\infty}^{\infty}\hat{a}(\omega_1)\hat{a}(\omega_2)\left[\int_0^{\Delta t} e^{-i(\omega_1+\omega_2)t}dt\right]d\omega_1 d\omega_2 ds_j\end{aligned}$$

Now using our earlier assumption that the time Δt between pulses is very long, we can use a property of the Dirac delta function

$$\int_{-\infty}^{+\infty} e^{-i\omega t}dt = \delta(\omega) \qquad (11)$$

to simplify further:

$$\begin{aligned}\int_S\int_0^{\tau} E_i D_j dt ds_j &= \varepsilon_r\varepsilon_0\int_S\mathscr{E}_i\mathscr{E}_j\int_{-\infty}^{\infty}\int_{-\infty}^{\infty}\hat{a}(\omega_1)\hat{a}(\omega_2)\delta(\omega_1+\omega_2)d\omega_1 d\omega_2 ds_j\\ &= \varepsilon_r\varepsilon_0\int_S\mathscr{E}_i\mathscr{E}_j\int_{-\infty}^{\infty}\hat{a}(\omega_1)\hat{a}^*(\omega_1)d\omega_1 ds_j\end{aligned}$$

where we used Hermitic symmetry $\hat{a}(\omega_1) = \hat{a}^*(-\omega_1)$ because $a(t)$ is real. Note that $\hat{a}(\omega_1)$, the laser's spectrum, is multiplied by its complex conjugate, eliminating any contributions from the laser's spectral phase. This means that the $E_i D_j$ term in equation (9) depends only on the magnitude of the laser pulse's spectrum, not on its phase. This is valid for each one of the terms in equation (9). Therefore, the spectral phase (or equivalently temporal shape or duration) of the pulse does not affect the average optical trapping force. These conclusions are supported by the numerical simulations and experimental work presented below.

In these arguments, our primary interest has been to determine whether pulse duration has any material-independent effect on optical trapping. We have therefore made a few assumptions about material properties such as refractive index, which are valid for the majority of materials, but to which interesting exceptions might be found. For example, we have assumed that the particle has not changed position or shape during the pulse's duration. Indeed, these effects propagate with the speed of sound while the optical pulse propagates with the speed of light,

#123223 - $15.00 USD Received 25 Jan 2010; revised 9 Mar 2010; accepted 11 Mar 2010; published 26 Mar 2010

and as such the particle is stationary during the duration of an ultra-short pulse[27]. We have also ignored material-dependent effects such as optical Kerr effects, optical gain, or damage to the trapped particle.

2.2. 2D simulation

In the previous section we have shown that, in the linear regime, the amount of impulse transferred from the optical pulse to the scattering objects is independent of the spectral phase of the pulse. Here, we visualise this effect by considering chirped pulses having the same spectra and defined by:

$$a(t) = \sqrt{T_0/T}\exp(-t^2/T^2)\cos\left(bt^2-\omega_0 t\right) \tag{12}$$

$$\hat{a}(\omega) = \frac{1}{2}\sqrt{\frac{T_0 T}{2-2ibT^2}}\exp\left(-\frac{T^2(\omega-\omega_0)^2}{4-4ibT^2}\right)+c.c. \tag{13}$$

where $b=\sqrt{T^2-T_0^2}/(T_0T^2)$ and where $c.c.$ stands for complex conjugate. The parameter T_0 corresponds to the time duration of the transform limited pulse which is the shortest pulse possible having the same spectral bandwidth. The parameter T gives the actual pulse duration including the spectral chirp.

For the numerical simulation, we consider the optical impulse transfer from a linear polarised pulse that has translational invariance in the z direction to an infinite cylinder with its axis also along the z direction. The pulse is focussed in the centre of the cylinder having an index of refraction $n=1.5$ in vacuum. The total force acting on the cylinder can be calculated by integrating the force density on the volume of the cylinder, V,

$$F_i(t) = \int_V (\partial_j T_{ij}-\partial_t g_i)\,dx^3 \tag{14}$$

Because of the translational invariance, this integral can be assessed by integrating on the area of the cross section of the cylinder and equating this with the force per unit length. Using this Maxwell's stress tensor approach as outlined above, and using vectorial notation to simplify the expressions, we calculate the time dependent total force acting on the object to be

$$\begin{aligned}\mathbf{F}(t) &= \int_V (\mathbf{D}\cdot\nabla)\mathbf{E}+(\mathbf{B}\cdot\nabla)\mathbf{H}-\frac{1}{2}\nabla(\mathbf{D}\cdot\mathbf{E}+\mathbf{B}\cdot\mathbf{H})-\partial_t\mathbf{g}\,dx^3 \\ &= \int_S (\mathbf{D}\cdot\mathbf{n})\mathbf{E}+(\mathbf{B}\cdot\mathbf{n})\mathbf{H}-\frac{1}{2}(\mathbf{D}\cdot\mathbf{E}+\mathbf{B}\cdot\mathbf{H})\mathbf{n}\,ds-\int_V\partial_t\mathbf{g}\,dx^3 \end{aligned}\tag{15}$$

where we arrived at the second form using numerical integration. Here, it is important to note that the integral needs to be calculated on the surface of the object using the fields outside the object.

To further verify our approach, we have implemented three additional methods to calculate the optical impulse transfer. The first two correspond to different ways to calculate the Lorentz force[28, 29] acting on the electric currents and charges due to the induced polarisation $\mathbf{P}=(\varepsilon_r-1)\varepsilon_0\mathbf{E}$.

$$\mathbf{F}(t) = \int_V (\mathbf{P}\cdot\nabla)\mathbf{E}+\partial_t\mathbf{P}\times\mu_0\mathbf{H}-\partial_t\mathbf{g}\,dx^3 \tag{16}$$

$$= \int_V -(\nabla\cdot\mathbf{P})\mathbf{E}+\partial_t\mathbf{P}\times\mu_0\mathbf{H}-\partial_t\mathbf{g}\,dx^3 \tag{17}$$

#123223 - $15.00 USD Received 25 Jan 2010; revised 9 Mar 2010; accepted 11 Mar 2010; published 26 Mar 2010

The third method can be seen as giving a different insight into where the momentum transfer actually takes place. Within this form, the momentum transfers only occurs at interfaces where light is scattered[30].

$$\mathbf{F}(t) \quad = \quad \int_V -\frac{\varepsilon_0}{2}(\mathbf{E}\cdot\mathbf{E})\nabla\varepsilon_r - \partial_t \mathbf{g}\, dx^3 \tag{18}$$

This expression can be generalised to the case of an absorbing object where additionally momentum transfer also occurs in the bulk material corresponding to the momentum loss due to the bulk absorption of the electromagnetic fields[31].

Finally, the time dependent momentum or impulse transfer for the pulse arriving around $t = 0$ is given by

$$\mathbf{S}(t) \quad = \quad \int_{-\Delta t/2}^{t} \mathbf{F}(\tau), d\tau \tag{19}$$

where we considered the integral of the instantaneous force from $\tau = -\Delta t/2$ (instant in the middle between two successive pulses) to the time instant t.

We calculate this time dependent impulse transfer for all four methods as shown in Figure 1, where we compare a transform limited pulse with a duration of 12fs to a chirped pulse with a duration of 40fs. Here, we have considered both the scattering force on the cylinder and the trapping force acting on the cylinder in the direction perpendicular to the direction of propagation of the pulse. We observe that these four methods of calculating the impulse transfer give the same total impulse with different transient behaviours. The origin of the variation is that each of the four different methods imply a different impulse transfer mechanism. In effect, each assume a different split between the momentum travelling with the electromagnetic fields and the momentum temporally stored in the material polarisation. Indeed, Maxwell's stress tensor approach corresponds simply to a momentum balance relation showing the impulse lost in the scattering process. In itself it does not give any insight on the mechanism of the momentum transfer. In contrast to Maxwell's stress tensor, the two versions of the Lorentz force and the surface force localise the instant and position of the momentum transfer. These three methods split the momentum inside the object differently, between the electromagnetic momentum and the momentum of the induced polarisation which travels together with the pulse but is not transferred to the object. In summary, we have used four different methods to calculate the time dependent impulse transfer, and have found that the total impulse (and therefore total trapping force) is the same regardless of pulse duration.

3. Experiment

3.1. Optical trapping experiment

We performed our experimental investigations of the effects of pulse duration on optical trapping using a homebuilt inverted optical trapping microscope (Figure 2). The trapping beam is an 80MHz Ti:Sapphire system from FemtoLasers (FemtoSource Scientific Pro), centered at approximately 800nm and capable of producing 12fs pulses. Before entering the trapping microscope, the beam passes through a 640-pixel one-dimensional spatial light modulating pulse shaper, custom built by Biophotonics Solutions, Inc. This pulse shaper is used to implement the Multiphoton Intrapulse Interference Phase Scan algorithm for dispersion measurement and compensation, as described in Section 3.2 below. The beam passes through a circular polarizer and is sent to the sample plane via a dichroic mirror. A 100x 1.40NA oil immersion objective (Nikon Plan Apo DIC H) forms the optical trap. Transmitted laser light from the sample plane is collected through a 0.65NA 40x Nikon E Plan objective, and loosely focused onto a quadrant

#123223 - $15.00 USD Received 25 Jan 2010; revised 9 Mar 2010; accepted 11 Mar 2010; published 26 Mar 2010

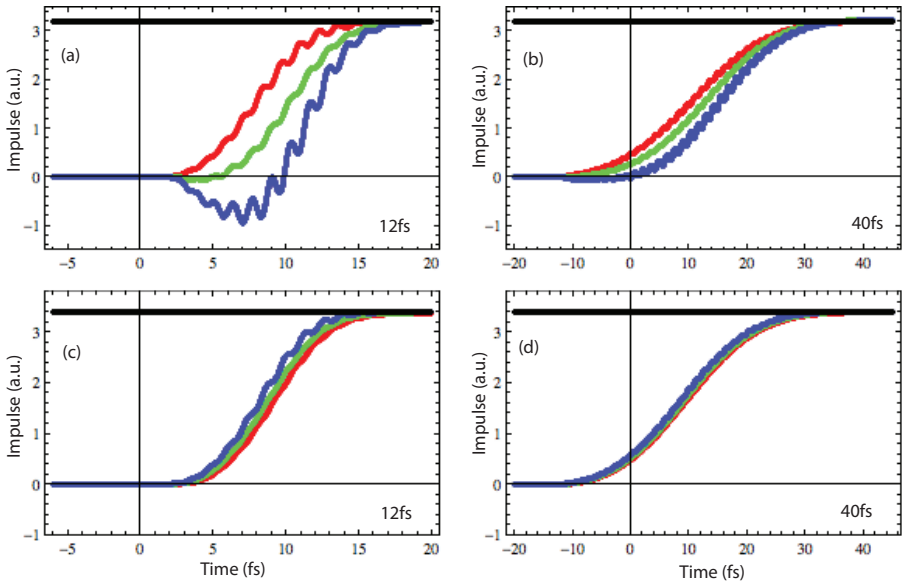

Fig. 1. Optical impulse transfer to a scattering cylinder by a 12fs (a,c) and a 40fs (b,d) Gaussian beam pulse, as a function of time. Red curves correspond to Maxwell's stress tensor integral (15), green to the first Lorentz force method (17) and blue to the surface force (18) and a second Lorentz force method (16) which are identical in this configuration. The black horizontal line corresponds to total impulse transfer per pulse, which is identical for all pulse durations and all calculation methods. (a,b) Impulse originating from the scattering force on a centred cylinder and (c,d) impulse originating from the radial trapping force calculated by displacing the cylinder laterally with respect to the axis of the beam.

photodiode (QPD) using a series of two lenses, for back focal plane interferometry-based position sensing[32]. The 40x objective also illuminates the sample from above, when desired; the dichroic mirror passes this illumination (as well as a small portion of back-reflected laser light) through a 200mm tube lens, which images the focal plane onto a CCD camera.

We also have the capacity to detect fluorescence from the trapped particles, used in our experiments on pulse shaping control of multiphoton excitation. Below the dichroic mirror is a 50/50 beamsplitter that sends half of the illumination/fluorescence to a spectrometer consisting of a Jobin-Yvon Triax 550 monochromator, coupled to a Jobin-Yvon Symphony Solo CCD camera. A demagnifying telescope consisting of a $f_1 = 200$mm and a $f_2 = 100$mm lens decreases the diameter of the signal beam by a factor of 2, and a short-pass filter (Comar GK 575) removes any remaining back-reflected laser signal. A 50mm lens focuses the signal onto the entrance slit of the spectrometer.

3.2. Dispersion measurement and compensation

To explore the effects of pulse duration on optical trapping, we need reproducible control over the temporal profiles of our pulses. Temporal dispersion is an effect by which laser pulses are stretched as they travel through optical media, owing to differences in refractive indices over the pulses' bandwidths. This effect is particularly dramatic for ultrashort pulses, whose durations can increase by several orders of maginitude by the time they reach the focal plane of a trapping microscope.

#123223 - $15.00 USD Received 25 Jan 2010; revised 9 Mar 2010; accepted 11 Mar 2010; published 26 Mar 2010

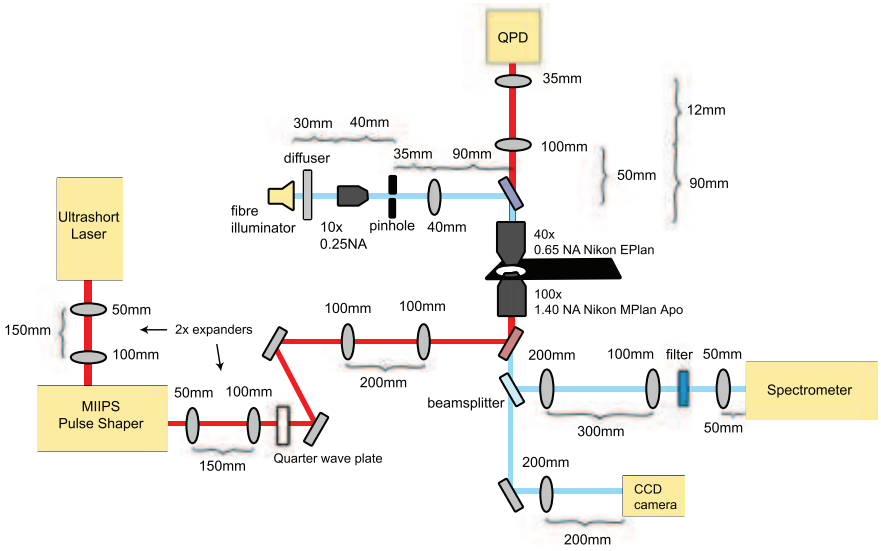

Fig. 2. Experimental setup, consisting of an ultrashort pulsed laser, a pulse shaper, and a homebuilt optical trapping microscope. The laser is a 800MHz 800nm Ti:Sapphire system capable of producing 12fs pulses. Before entering the microscope, the beam travels through a pulse shaper (BioPhotonic Systems, Inc), containing a 640-pixel spatial light modulator (CRi), used to implement the Multiphoton Intrapulse Interference Phase Scan (MIIPS) method of dispersion measurement and compensation. The optical trapping microscope has quadrant photodiode (QPD) position detection, white light illumination, CCD imaging, and a spectrometer for detection of fluorescence signal at the sample plane.

The dispersion in an optical system, if precisely known, can be compensated for by manually pre-dispersing the laser pulses with the opposite dispersion, so the net dispersion at the sample is zero. Measuring and compensating dispersion is not straightforward, due to the extremely short timescales involved and the complex wavelength dependence of refractive index for the various materials and coatings within an optical system. The problem is compounded for microscope systems, due to geometrical restrictions and the magnitude and complexity of dispersion these systems introduce. It has only recently been possible to completely compensate for all orders of dispersion in a microscope system.

We use the MIIPS (Multiphoton Intrapulse Interference Phase Scan) method[33, 34, 35] to measure and eliminate dispersion in our optical trapping microscope, achieving approximatively 12fs pulse durations at the sample plane. The MIIPS measurement requires a pulse shaper to be placed somewhere in the beam path before the sample plane, and a method to measure the laser's second harmonic spectrum at the sample plane. In our case, we use a thin BBO crystal to generate the second harmonic and a fiber spectrometer (Ocean Optics) for the spectral measurement. The measurement must be repeated every time optics are added or removed from the beam path, as well as at least daily to compensate for shifts in the laser cavity's dispersion. The successful elimination of dispersion in our optical trapping system, representing the first use of MIIPS in an optical trapping system as well as the shortest pulse duration used for optical trapping by an order of magnitude, has been described elsewhere[36]. Compared to our uncompensated pulses, our dispersion-compensated pulses are shorter by roughly two orders of magnitude. Although average power remains the same, the dispersion compensated pulses

#123223 - $15.00 USD Received 25 Jan 2010; revised 9 Mar 2010; accepted 11 Mar 2010; published 26 Mar 2010

produce nonlinear signal that is much higher and more reproducible[36]. In this work, we use the dispersion-compensated pulses as a starting point for our pulse shaping experiments.

3.3. Pulse shaping

Starting from dispersion-compensated pulses as a blank slate, we use the MIIPS pulse shaper to reproducibly control the pulse temporal profile at the trapping plane. The range of pulse shapes that we could implement in this fashion is almost limitless; in these studies, our aim was to decrease peak power while leaving the pulse's average power and spectrum unchanged.

The most straightforward method of stretching the pulse is to add positive or negative 2nd order dispersion (also known as GVD, or a quadratic phase function). The advantage of using 2nd order dispersion to increase pulse duration is that the time profile is stretched without changing shape; likewise, the efficiency of multiphoton excitation is decreased monotonically for all wavelengths.

We calculated the pulse durations resulting from various amounts of 2nd order dispersion using inverse Fourier transform, given the test phase function and the fundamental spectrum of the laser. We chose 2nd order dispersion amounts that would produce pulse durations approximately evenly spaced in log scale; these phase functions are of the form $\phi(\omega) = \frac{1}{2}\gamma_2(\omega - \omega_0)^2$, where γ_2 is the amount of 2nd order dispersion in fs^2, and ω_0 is the centre frequency of the phase function. In our case, ω_0 was chosen to be 2.48 10^{15} rad/s (corresponding to $\lambda_0 = 759.11nm$). Table 1 shows the γ_2 used, along with the resulting pulse durations.

$\gamma_2(fs)^2$	Duration (fs)
0	12.9
96	20.0
117	30.0
180	50.2
242	70.0
337	99.9
625	200.0
1530	500.2

Table 1. Amount of 2^{nd} order dispersion used to produce desired pulse durations. γ_2 is the amount of 2^{nd} order dispersion in fs^2, and ω_0 is the centre frequency of the phase function. In our case, ω_0 was chosen to be $2.48 * 10^{15}$rad/s (corresponding to $\lambda_0 = 759nm$). The resulting FWHM pulse duration (assuming a roughly Gaussian time profile) is calculated using inverse Fourier transform.

3.4. Effect of pulse duration on measured trap stiffness

For each pulse duration produced as described in Section 3.3, we trapped single 780nm diameter silica particles at 47mW average power, as measured at the sample plane using the double objective method[37]. The positions of the trapped silica particles were monitored over 6.7 consecutive seconds at an acquisition rate of 30,000 samples/second for each of the four quadrants of the QPD. This position measurement was repeated six consecutive times for each of three different silica particles (giving a total combined acquisition length of 40 seconds for each particle). We used our own Mathematica program to calculate the power spectra in x, y, and z of each 40 second acquisition and fit a Lorentzian curve to these power spectra. For a description of the power spectrum fitting, as well as example power spectra, see reference [36].

#123223 - $15.00 USD Received 25 Jan 2010; revised 9 Mar 2010; accepted 11 Mar 2010; published 26 Mar 2010

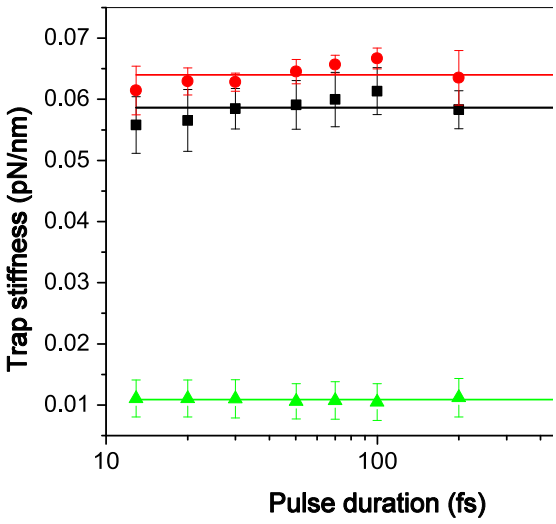

Fig. 3. Measured trap stiffness of 780nm diameter silica particles in the x, y, and z directions, trapped in 3D using a pulsed 780nm Ti:Sapphire laser. Each data point shows the average of a 40 second acquisition for each of three trapped particles. Pulse duration was varied from 12fs to 500fs using positive 2^{nd}-order phase modulation in addition to a phase function that compensated the measured dispersion of the system. For all measurements, the average power at the sample plane was 47mW. The lines show the trap stiffness (fN/nm): x: 58.6±0.6, y: 64.1±0.6, z: 10.9±0.1. The fluctuations of the trap stiffness are about 10% over the whole range of pulse duration considered.

We repeated this measurement for three particles, and the average trap stiffness in x, y, and z for these three trials is shown in Figure 3.

From Figure 3, it is evident that although pulse duration was changed by roughly 1.5 orders of magnitude, trap stiffness remained unchanged to within 10%. Trap stiffness in the x and y (transverse) directions increased slightly, but this increase is very close to the fit error. Trap stiffness in the z (axial) direction was unchanged within experimental error. Average power remained the same in all cases. This observation indicates that in the absence of material-dependent effects, optical trapping in x, y, and z depend on average power rather than peak power.

We remark, here, that our theoretical approach and experimental observation lead to a different conclusion than the one reached by Wang et al[22]. This can easily be explained when considering the difference between instantaneous force and impulse transfer from a laser pulse. Fig. 4a shows the peak axial force acting on a Rayleigh particle originating from a Gaussian laser pulse. For this simulation, we used the same parameters and theoretical framework as the one presented by Wang et al[22] and indeed our results show exactly the same theoretical curve as figure 2h in reference[22]. Here, we chose to represent the peak force in a log-log scale highlighting the inverse proportional relation between peak force and pulse duration. Indeed, the peak force has the same behaviour as the peak power of a pulse while the momentum transfer the same behaviour as the energy of a pulse. This explains their inverse proportional relationship. Further, using the same parameters and formalism, we can calculate the time dependence

#123223 - $15.00 USD Received 25 Jan 2010; revised 9 Mar 2010; accepted 11 Mar 2010; published 26 Mar 2010

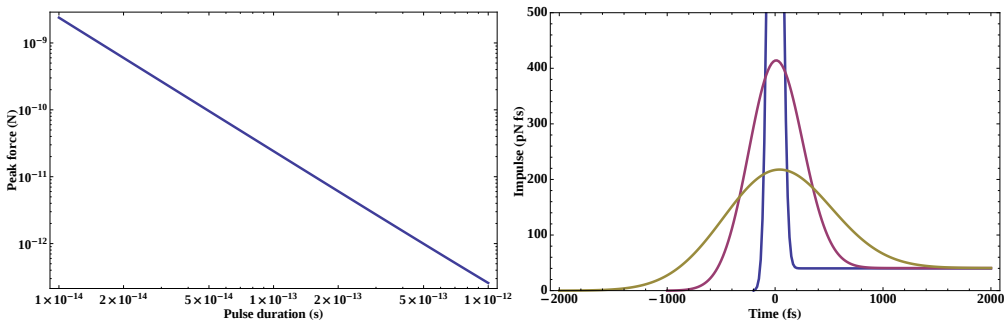

Fig. 4. Optical impulse transfer to a Rayleigh particle in water using the same parameters as reference [22]. (a) Peak force as a function of pulse duration showing an inverse-proportional relationship. (b) Axial impulse transfer to the same Rayleigh particle as a function of time for pulses of 100fs, 500fs and 1ps showing that regardless of the pulse duration, the total momentum transfer is the same.

of the impulse transfer. Fig. 4b shows that regardless of the pulse duration the total momentum transfer is constant but the duration over which this is achieved is different leading to different peak forces. It is this fundamental misunderstanding that leads to different interpretation of the same phenomena.

To understand the apparent experimental validation of the dependance of the optical force on pulse duration presented elsewhere[19,23], one needs to take into account the optical and mechanical non-linear properties present in the experiment. These properties are due, either to a non-linear response in the time domain, such as Kerr lensing or fluorescence saturation or from the change of the optical spectral bandwidth with pulse duration or from the frequency bandwidth of the instantaneous force. In the latter case, the Fourier transform of a force originating from an ultrashort pulse will include high frequency components probing a different frequency range of the mechanical response of a system. Using this argument, one can imagine accessing, in the ultrashort pulse regime, some "mechanical" resonance of the system effectively breaking the cohesion of particles to the interface[19]. Changing the spectral bandwidth of the beam has a similar effect. Indeed, fluorescent particles, such as the ones used by De et al. [23], absorb and re-emit light at a different wavelength changing the spectral bandwidth of the optical interaction in a non-linear fluorescence process. This process might explain the trapping behavior observed by De et al[23].

3.5. Pulse shaping for control of nonlinear processes in optically trapped particles

The absence of a trapping dependence on pulse time profile gives us the freedom to modulate ultrashort pulses to control multiphoton effects in trapped Lorentz-Mie particles. In this work, we use quadratic pulse shaping to control two-photon excitation in 3D trapped particles. We trapped blue fluorescently-dyed 2.1μm diameter polystyrene spheres (B0200 from Duke Scientific/Thermo Scientific), which absorb two-photon excitation from a wavelength range within our laser's SHG bandwidth (380-420nm). The back-reflected fluorescence signal, stretching from approximately 420-580nm, is collected using a spectrometer (Figure 2).

The white-light illumination wavelengths overlapped the fluorescence signal, so illumination had to be turned off whenever fluorescence was being collected. Photobleaching effects meant that fluorescence measurement had to start immediately after the particle was trapped. To achieve this, we diluted the sample, and located (but not trapped) individual particles with

#123223 - $15.00 USD Received 25 Jan 2010; revised 9 Mar 2010; accepted 11 Mar 2010; published 26 Mar 2010

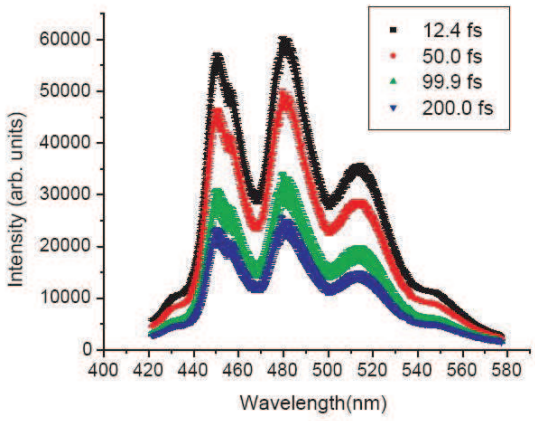

Fig. 5. Control of two-photon fluorescence in 3D trapped 2.1μm blue fluorescently-dyed polymer particles. Two-photon fluorescence spectra were measured with four different pulse durations, with pulse duration varied by introducing 2nd order dispersion with a pulse shaper. The same average power (3mW) was used for all measurements. We remark that the two photon fluorescence saturates for such ultrashort pulses and the position of the spheres may vary between measurements.

the aid of illumination. Once we had located a particle, we switched off the illumination and moved the sample so the particle was close enough to jump into the trap. The presence of the particle in the trap was verified by fluorescence signal visible on the CCD camera, and fluorescence spectral acquisition started within 1s.

The polymer particles were ablated and pushed along the beam at powers above 3.7mW when we used dispersion-compensated 12fs pulses. At powers above 15mW, the particles would be ejected axially from the trap almost immediately, and exhibited large shape deformations and craters. At powers between 3.7mW and 7mW, the particles could be trapped for up to a few minutes (depending on the quality of laser alignment into the microscope system) until they were suddenly ejected axially from the trap. Imaging of these particles revealed that they had been drilled with narrow holes, an effect similar to that observed by Misawa and coworkers[6]. When we used pulse shaping to produce longer pulses with lower peak power, the ablation effect was lessened and the particles could be stably trapped for much longer. At powers between 1.8mW and 3mW, not far above the threshold where the 2.1μm particles could be trapped, the particles could be trapped for several minutes at 12fs pulse duration with no visible damage. In our experiments we used the lowest-power regime, with an average power of 3mW at the sample plane.

As in Section 3.4, we first compensated for the dispersion already on the system, then used additional positive 2nd order dispersion to control pulse duration. For each pulse duration, we measured the fluorescence signal from a trapped particle over 5 seconds. To avoid photobleaching effects, we used a different particle for each measurement. For each pulse duration, we repeated the measurement with four different particles. The measured fluorescence spectra are shown in Figure 5. As expected, fluorescence intensity decreases as pulse duration increases. Note that because average power remained the same throughout the experiment, trap stiffness has remained invariant. In laser systems without a convenient method of rapidly switching between CW and mode-locked regimes, this method could be used to switch between a long pulse duration that avoids photobleaching and a short pulse duration that maximises fluorescence sig-

#123223 - $15.00 USD Received 25 Jan 2010; revised 9 Mar 2010; accepted 11 Mar 2010; published 26 Mar 2010

nal. This paper demonstrates just one possible method of multiphoton control in trapped particles. With other pulse shaping techniques, more advanced forms of control are possible. Some example applications include low-background single-beam coherent anti-Stokes Raman scattering (CARS) [38], highly accurate refractive index measurement [39], precise measurement of two-photon excitation spectra [40], and selective multiphoton excitation without wavelength tuning or filters [41].

4. Summary and conclusions

We have found through theory, numerical simulation, and experiment that linear optical trapping using pulsed lasers is independent of the pulse's duration or time profile. Our generic theory and numerical simulation results give strong evidence that there is no pulse duration effect neither in the Rayleigh regime nor in the Lorenz-Mie, once we take into account the total force applied by the laser over the repetition cycle.

For our theoretical investigations, we examined the equations for trapping using high repetition rate, short pulsed lasers, and found that the pulse's field is multiplied by its complex conjugate, eliminating any dependence of trapping on the pulse's time profile. This means that, in the linear regime, the amount of momentum transfer is independent of the pulse duration for pulses with equivalent spectra. We performed numerical simulations using four different methods and found that the total momentum transfer was the same for 12fs pulses and for 40fs pulses.

For experimental verification of these results, we trapped 780nm diameter silica particles in 3D with an 80MHz pulsed laser source, using dispersion compensation to compress our pulses to 12 femtosecond FWHM duration at the trapping plane. With the compensated pulses as a starting point, we used pulse shaping to systematically vary the pulse duration over 1.5 orders of magnitude, while keeping average power and spectral content unchanged. We found no significant effects of pulse duration on optical trapping. Additionally, it is possible to use phase shaping to control nonlinear processes in optically trapped particles without affecting optical trapping itself. This was demonstrated by using 2nd order phase functions to increase pulse duration, and observing the effects on two-photon fluorescence in trapped dyed polymer spheres. Two-photon fluorescence decreased as pulse duration increased, as expected. The use of pulse shaping in combination with optical trapping opens the door to other forms of controlling multiphoton effects in trapped particles, or spectroscopic methods such as single-beam CARS.

Our theoretical and experimental investigations were designed to eliminate any material-dependent effects on optical trapping. However, pulse duration-dependent effects exist for some materials, and may make interesting subjects for future investigations. One of the easiest-to-observe effects is that of multiphoton damage to the trapped particle, sometimes in combination with self-focusing, which for materials such as polystyrene may disrupt the trapping process or even destroy or deform the particle. Other effects such as the presence of optical Kerr effect, or optical gain guiding may also be noticeable in some materials. Pulse shaping control of the trapping laser's temporal profile may enable interesting studies in these areas.

Acknowledgements

The authors are grateful to the UK Engineering and Physical Sciences Research Council (EPSRC) for funding. MM acknowledges support from Scottish Enterprise. JS was supported in part by a USA National Science Foundation Graduate Research Fellowship. We are grateful to BioPhotonic Solutions Inc for making available to us one of their first MIIPS Box 640 phase amplitude pulse shapers. We thank Dr. Pastirk from BioPhotonic Solutions and Prof. M. Dantus for their support with the MIIPS pulse compression technique and Prof. M. Dantus for useful comments on the manuscript. KD is a Royal Society Wolfson Merit Award Holder.

#123223 - $15.00 USD Received 25 Jan 2010; revised 9 Mar 2010; accepted 11 Mar 2010; published 26 Mar 2010